JOURNAL OF ENERGY SYSTEMS

2022, 6(2)

2602-2052 DOI: 10.30521/jes.1123925 Research Article

The simulation of a new high frequency transformer

Sude Hatem
Gazi University, Graduate School of Science and Technology, Department of Electrical and Electronics Engineering, Ankara, Türkiye, sude.hatem@gmail.com
Erol Kurt
Gazi University, Technology Faculty, Department of Electrical and Electronics Engineering, Ankara, Türkiye, ekurt@gazi.edu.tr

Submitted: 01.06.2022
Accepted: 13.06.2022
Published: 30.06.2022

Abstract: Core losses of transformers motivate many engineers and scientists to design and implement different transformers for their specific aims. Since there exists a growing interest on high frequency applications in today's world, design and optimization studies of a magnetic fluid core transformer (MFCT), having an easy and cheap production approach in high frequency applications, are considered in the present paper. The desired design should operate in a more efficient way within a wide frequency band. The MFCT considered here can be a solution to the eddy currents and core losses encountered in the conventional transformers with its low conductivity, oil-based magnetic fluid and super paramagnetic characteristic. The magnetic fluid in the proposed work consists of a combination of ferromagnetic particles made by iron in an averaged diameter of 70 μm with an adjustable magnetism compared to the traditional magnetic fluids and an engine oil, thereby the magnetic permeability of the overall fluid core can be fully adjustable by the variation of mass proportion between the oil and iron powder as an easy process without any chemical process. A COMSOL Multi-Physics design is performed via a finite element package in three dimensions. It is proven that the iron particles exhibit a complicated pattern inside the engine oil and produce a well-defined high frequency output at the secondary windings in a wide range of frequency.

Keywords: *Core, Ferrofluid, High frequency, Magnetic fluid, MHz, Power, Transformer*

Cite this paper as: Hatem, S., & Kurt, E., The simulation of a new high frequency transformer. *Journal of Energy Systems* 2022; *6*(2): 322-337, DOI: 10.30521/jes.1123925

1. INTRODUCTION

The most efficient distribution transformers providing continuous service (except for interruptions during maintenance and breakdown) operate with a loss of approximately 3% of the electricity they transmit. The industrial subsidiaries are constantly researching new methods and technologies to reduce operating costs and energy losses. After the invention of transformers, the selection of suitable materials in the production of the core has been intensely considered since that seriously affects the performance of the transformers. A proper core material can reduce losses at high flux density (B), while enabling the transformer to operate at the desired frequencies (f). With high power density (p), lightweight and the increasing trend towards high efficiency inverters, magnetic components have an important role in achieving all the above-mentioned characteristics. Especially, with the advent of high-frequency switching components, the electrical elements such as transformers and coils can operate effectively at higher operating frequencies such as KHz and MHz with smaller sizes. However, these miniature dimensions contain additional losses [1]. Therefore, the selection of magnetic elements is important in order to achieve minimum parasitic output and maximum efficiency in high operating frequency devices. Choosing the correct core will primarily protect the transformer from overheating due to core loss. During the optimal design, it is important to keep different material properties such as resistivity, magnetic saturation and electrical permeability in balance [2].

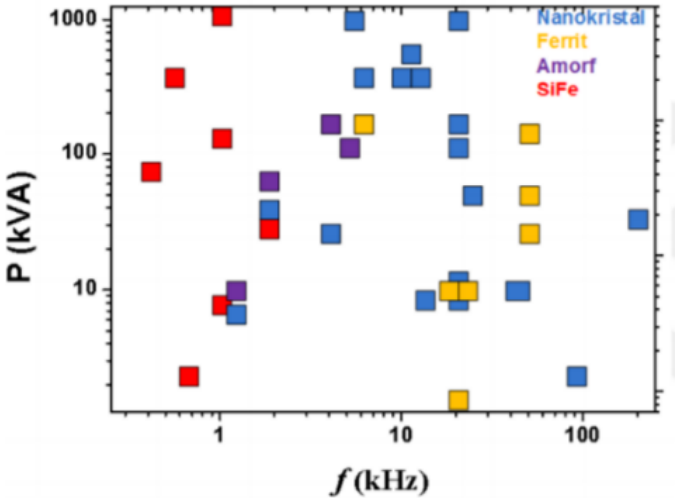

Figure 1. Power-frequency characteristics of soft-core materials [3].

Fig. 1 represents the power-frequency logarithmic graph for transformers made of different core materials currently used in the literature and industry. According to this graph, cores produced from nanocrystalline materials exhibit a uniform distribution in terms of frequency (f) and power (P) characteristics, while cores with SiFe material are preferred at low frequencies, and amorphous cores are preferred at mid-low frequencies and relatively low powers. On the other hand, ferrite structures are in the same status as amorphous in terms of power, while they can reach higher frequencies (about 14 kHz). Transformers operating at 100 kHz frequencies can be encountered with nanocrystal applications. With increasing operating frequency, more magnetic materials have been introduced for several applications.

Magnetic core structures vary depending on the application and the topology of the system. While different steel lamination grades were used before, with the addition of 4-5% silicon for steel, it is possible to reduce the eddy currents and hysteresis losses to some extent, and thus to increase the performance and efficiency of the transformer, with the addition of 4-5% silicon for steel [4,5]. Iron

alloys, amorphous materials, soft magnetic ferrites and iron powders are the main groups of core materials for commercially available transformers.

The ferrofluid core transformer is appropriate for a prototype solution to eddy currents and hysteresis losses (core losses), with its low electrical conductivity and superparamagnetic properties of oil-base. The weight lightness and magnetization rate of transformers are two important factors influencing their performance. Therefore, the use of magnetic liquid materials can be preferred in the core of electromagnetic systems working for special purposes. Actually, the electrical properties and output characteristics of designed magnetic fluid core transformer (MFCT) is similar to the solid core transformers used industrially and it is preferred in different fields and applications such as defense industry and medicine due to its high efficiency, longer lifespan, miniature structure, lightness and high magnetization of the core. The creation of the ferrofluid used as MFCT's core needs several stages. Hence, an easier approach for ferrofluid production can be preferable, less time consuming and cheaper. In this research, a simple, inexpensive and efficient method for using ferrofluid as transformer core is introduced and implemented by experimental studies.

In Section 2, the theory of the proposed transformer model containing a liquid core is explained and the mathematical model is defined. Methodology of the research is described in Section 3. The definition of the ferrofluid used as MFCT's core and numerical simulation results for various concentrations of nanoparticles floated in oil base are presented in Section 4. Finally, in Section 5 the conclusion of the study is explained.

2. THEORY

In high frequency applications, electromagnetic fields have the function of carrying energy in all electromagnetic environments. Therefore, both precise analytical and numerical analyses of the electromagnetic fields are important tasks for the examination of the properties of these devices and systems. When an external magnetic field (*H*) is used, the magnetic dipoles in a ferrofluid are oriented in the same direction. Otherwise, they are randomly oriented without obtaining a net magnetization. When an agitation occurs in the fluid, a complex fluid motion involving large amplitude surface waves occurs. This turbulent action changes the direction of the magnetic dipoles during the agitation causing sudden changes in the magnetic flux. This effect induces an electromotive force (*EMF*) in the outside of the container when a coil is wrapped on the container. The main difference between a solid core and a ferrofluid is that the ferrofluid contains an infinite number of modes due to its turbulent motion. For the design of the mathematical model, the *H* source should initially be modeled. Then the magnetic field is calculated and the magnetization body forces are evaluated. Finally, the flow in the liquid core is analyzed. Electric currents are a static problem for the electric field inside the coil by the mathematical model in the windings (magnetic field source).

$$\nabla.(\sigma \nabla V_e) = 0\,, \tag{1}$$

where, V_e [V] is the electrokinetic potential. The terminals of each coil specify Dirichlet boundary conditions (voltage at one end, ground at the other) depending on the power scheme and σ [*S/m*] defines the electric conductivity. After calculating the current density, the static magnetic field solver solves the following expressions using Ampere's Law and Maxwell's equations:

$$\nabla \times \vec{H} = \vec{J_e} + \vec{J_o} \tag{2}$$

$$\nabla \cdot \vec{B} = 0 \tag{3}$$

$$\nabla . \vec{D} = \rho \tag{4}$$

Here, $\vec{H}$ (x,y,z), $\vec{B}$ (x,y,z), $\vec{J_e}$, $\vec{J_o}$, $\vec{D}$ and ρ are magnetic field strength (A/m), magnetic flux density (T), eddy current density (A/m^2), external current density (A/m^2), electric flux density (C/m^2) and charge density (C/m^3), respectively. The relation between the magnetic flux density and field strength is given by,

$$\vec{B} = \mu_r \, \mu_0 \, \vec{H} \tag{5}$$

Where μ_r (x,y,z) is the relative permittivity, and μ_o $=4\pi 10^{-7}(H/m)$ stands. The system calculates the moment about the x, y, z axis using the Lorentz force:

$$T = \int \vec{r} \times (\vec{J} \times \vec{B}) dv \tag{6}$$

Here r is the displacement vector in the rotation axis. Boundary condition of electrical insulation is,

$$n \cdot \vec{J} = 0 \tag{7}$$

n is the outward normal. Here, the voltage drop on each coil is adjusted so that the electric current density in the coils is 1 A/mm^2. The resulting current density is defined as an external field source to the magnetic field problem. The analysis of inductances is based on the mathematical model for the magnetic field. In copper windings and in free space:

$$\nabla \times (\mu_0^{-1} \mu_r^{-1} \nabla \times \vec{A}) = \vec{J_e} \, , \tag{8}$$

stands. In ferrofluid core, due to magnetization M,

$$\nabla \times (\mu_0^{-1} \mu_r^{-1} \nabla \times \vec{A} - \vec{M}) = 0, \tag{9}$$

is written. Here, $\vec{A}$ is the magnetic vector potential and $\vec{M}$ is the magnetization in the magnetic nanofluid and with the analytical formula which it is approximately:

$$M = \gamma \, arctan(\lambda H) \tag{10}$$

Here, γ and λ are the experimental constants chosen to exactly match the experimental magnetization characteristic of the magnetic fluid. As theoretical equations,

- *Conservation of momentum:*

$$\rho \, (\vec{u} \cdot \nabla)\vec{u} = \nabla \cdot \left[-pI + \eta \, (\nabla \overrightarrow{|u|} + \nabla \overrightarrow{|u|})^T\right] + f_{mg} - \rho g \tag{11}$$

- *Mass conservation:*

$$\nabla \cdot \vec{u} = 0 \tag{12}$$

- *Turbulent kinetic energy transportation:*

$$\rho\vec{u}\cdot\nabla k = \nabla\cdot[(\eta + \sigma_k\eta_T)\nabla k] + \eta_T P(u) - \beta_k\rho k\omega \quad (13)$$

- *Turbulent frequency transportation:*

$$\rho\vec{u}\cdot\nabla\omega = \nabla\cdot[(\eta + \sigma_\omega\eta_T)\nabla\omega] + \propto \omega\,\eta_T P(u)/k - \beta_k\rho\omega^2 \quad (14)$$

The ferro-fluid behavior is explained by solving the formulas together. Here *u* is velocity, *p* pressure, ρ mass density, *g* gravitational acceleration, and η is dynamic viscosity.

$$f_{mg} = \mu_0\,(\vec{M}\cdot\nabla)\,\vec{H} \quad (15)$$

Here f_{mg} is defined as magnetization external force in N/m^3 [2,6]. The pressure and turbulent viscosity are given by,

$$P(u) = \nabla\cdot\vec{u}[(\nabla\cdot\vec{u} + \nabla\cdot\vec{u})^T], \quad (16)$$

and,

$$\eta_T = \rho k/\omega. \quad (17)$$

Here, ω $[m^2/s^3]$ is the turbulent frequency. The modeled magnetic nano-fluid, is considered as a Newtonian, homogeneous and isotropic fluid.

3. METHODOLOGY

All designs of the MFCT subjected to this article, are realized through COMSOL Multi-physics package program, which uses the three-dimensional finite element method. From the modeling point of view, a transformer basically has a 3D geometry. The application of the 3D finite element method to the design of electrical machines allows determination of important design parameters such as the encircled flux, current density, winding inductances and the generated electromagnetic field with very high accuracy. In the preferred program, in case the properties of the materials and the boundary conditions are entered correctly, the reactions of the system in various situations can be determined beforehand [7]. For the vast majority of geometries and problems PDEs (partial differential equations) cannot be solved by analytical methods. Instead, an approximation of the equations can be constructed, typically based on different kinds of discretization. These discretization methods approximate PDEs with numerical model equations that can be solved by numerical methods. The solution of numerical model equations, in turn, is an approximation of the real solution to PDEs. The finite element method (FEM) is used to calculate such approximations. [8,9]. Fig. 2 provides the COMSOL geometric design of the transformer subjected to this paper.

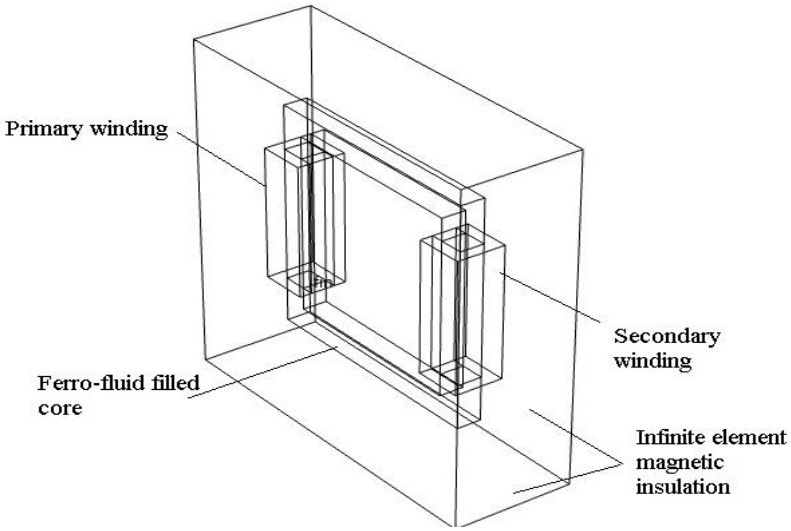

Figure 2. The 3D design of the transformer.

4. NUMERICAL SIMULATION WITH THE PROPOSED FERROFLUID

In order to define the considered ferrofluid material properties of MFCT's core, the characteristics and physical parameters given in Table 1 are applied and the *B-H* curve of the ferromagnetic particles is introduced to the defined material by adding a specific constitutive *B-H* relation. As a result, the magnetic field norm would need a definition depended on the *B-H* curve, hence reaching both properties of fluidity and ferromagnetism are possible. In order to design and evaluate magnetic body forces and observe the magnetic flux intensity of flow patterns of velocity field through the MFCT's core, magnetic fields and computational fluid dynamics (CFD) modules are used physics in simulation program of Comsol Multi-Physics v6.5.

Table 1. Physical parameters of engine oil-based ferro-fluid used in simulation model.

Parameter	Description
Dynamic viscosity (Pa.s)	0.15
Density (g/cm^3)	1.21 – 7.104
Heat capacity at constant pressure J/(kg·K)	1.67
Thermal conductivity (W/mK)	0.176
Electrical conductivity [MS/m]	10^{-12}
Chemical composition of magnetic particle	Fe
Magnetic particle mean radius[μm]	70
Magnetic particles weight concentration	0.1-0.9
Operating frequency [MHz]	1-20

The Galerkin finite element method (FEM) is used to solve the problem. Meshing sequence, which is added to the model, is calibrated as fluid dynamics for ferrofluid core domain and general physics for the remaining geometry of MFCT. The generated mesh is presented in Fig. 3.

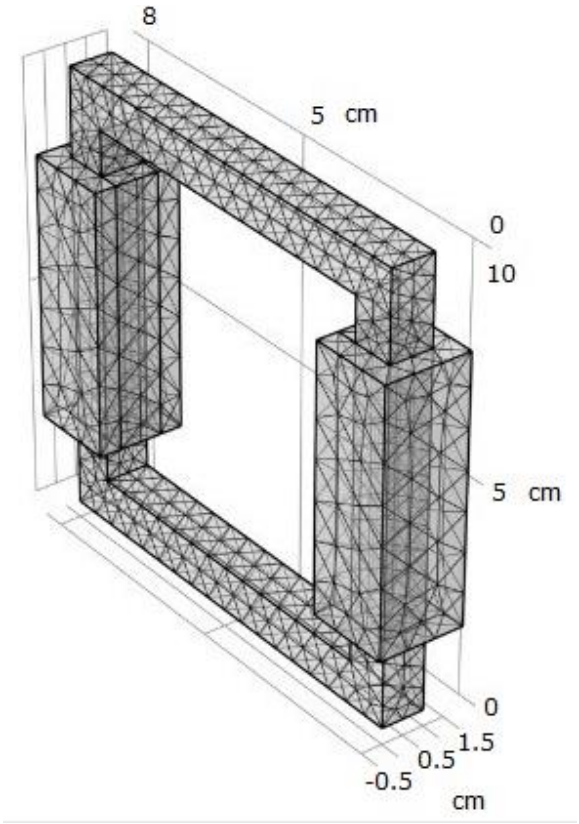

Figure 3. The meshed structure.

The Eqs. (7-9) can be solved if the magnetic field source is identified. In the numerical simulations, the field is modelled using tetrahedral, quadratic vector elements. Because of the nonlinear behavior of the ferrofluid core, the algebraic problem relating to the FEM analysis is nonlinear. As a result, in order to improve sequential and parallel sparse numerical factorization performance, the MUMPS solver algorithm is preferred with a combination of left-looking and right-looking super node techniques. According to various average mass concentration of dispersed nanoparticles, the density of mixture consisting of iron powder nanoparticles and engine oil is calculated and presented in Table 2.

In the first phase of operation, in order to visualize the magnetic flux density produced, the simulation process is carried out for a MFCT core with $\rho = 4336.25$ [kg/m^3] mixture density, which corresponds to about 50% nanoparticles mass fraction. The magnetic flux density spectrum and flowing flux of simulated MFCT by three powering schemes are indicated in Fig. 4 through flux lines. The first scenario is powering only the primary winding, the second scenario is powering only the secondary winding and the third one is powering both windings with additional flux excitation. The simulation results for the above-mentioned two processes are presented via graphics and plots.

Table 2. The magnetic nanoparticles and engine oil mixture density for various particles mass fractions.

Nanoparticles concentration (φ_d) %	**Mixture density** (ρ) [kg/m^3]
5	1218.87
10	1565.25
20	2258
30	2950.75
40	3643.5
50	4336.25
60	5029
70	5721.75
80	6414.5
90	7104.8

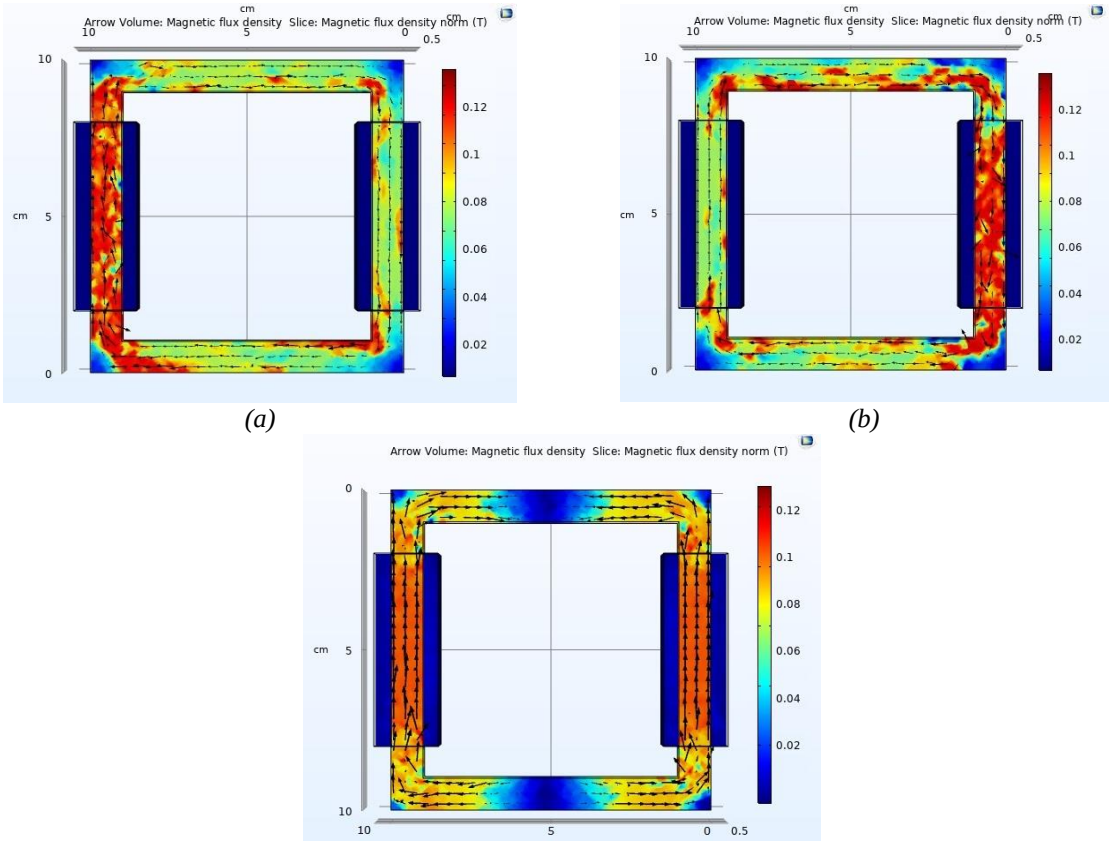

Figure 4. The magnetic flux density spectrum and flowing flux: a) Primary winding is powered on b) Secondary winding is powered on, c) Both windings are on with the same current excitation

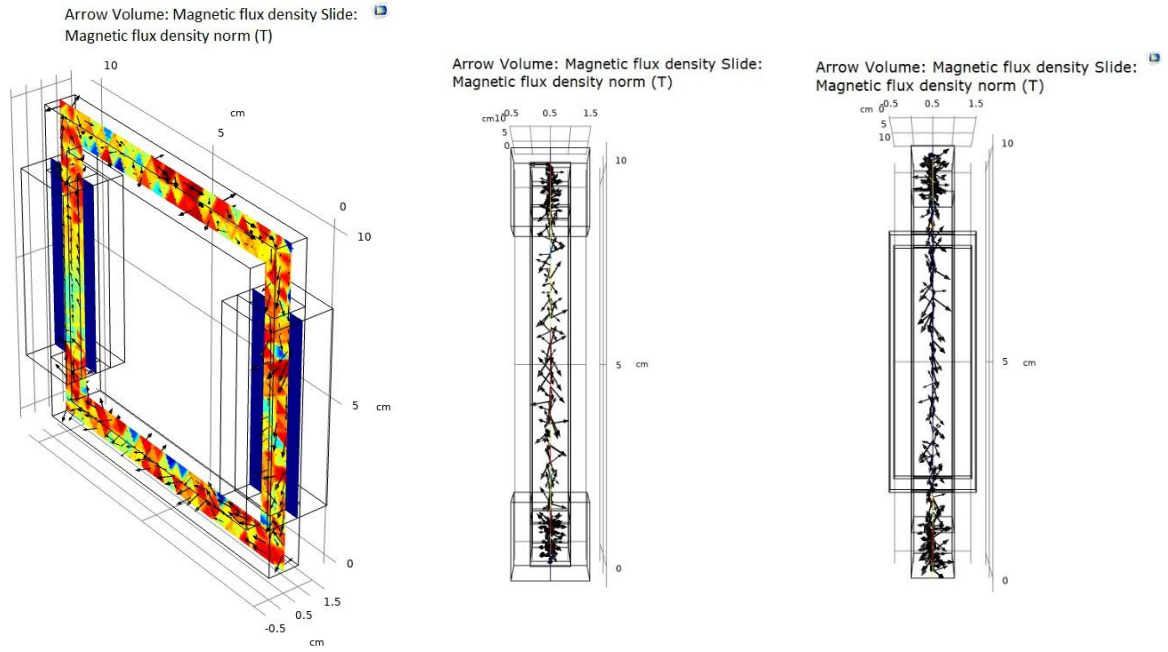

Figure 5. The magnetic flux densities of the flowing flux: a) Secondary winding is powered on, a) in 3D appearance, b) x-z plane coordinates, c) x-y plane coordinates.

The results for the case when secondary winding is powered are presented for 3D, *x-z* and *x-y* planes in Fig. 5. The color and size of the lines are proportional to the value of the magnetic flux density of model. According to the reported results, when there is no magnetic field applied, the magnetic dipoles in the ferrofluid are oriented in the same direction, instead of their random orientations. Hence, no magnetization exists. When an external magnetic field is applied and a very small agitation is occurred in the fluid, a complicated fluid motion involving large amplitude surface waves occurs. This turbulent action changes the direction of the magnetic dipoles, which causes sudden changes in magnetic flux. The influence of the external magnetic body forces on magnetization of ferrofluid core is observed by numerical simulation. In addition, the magnetic permeability variation of core with respect to varying time is presented in Fig. 6.

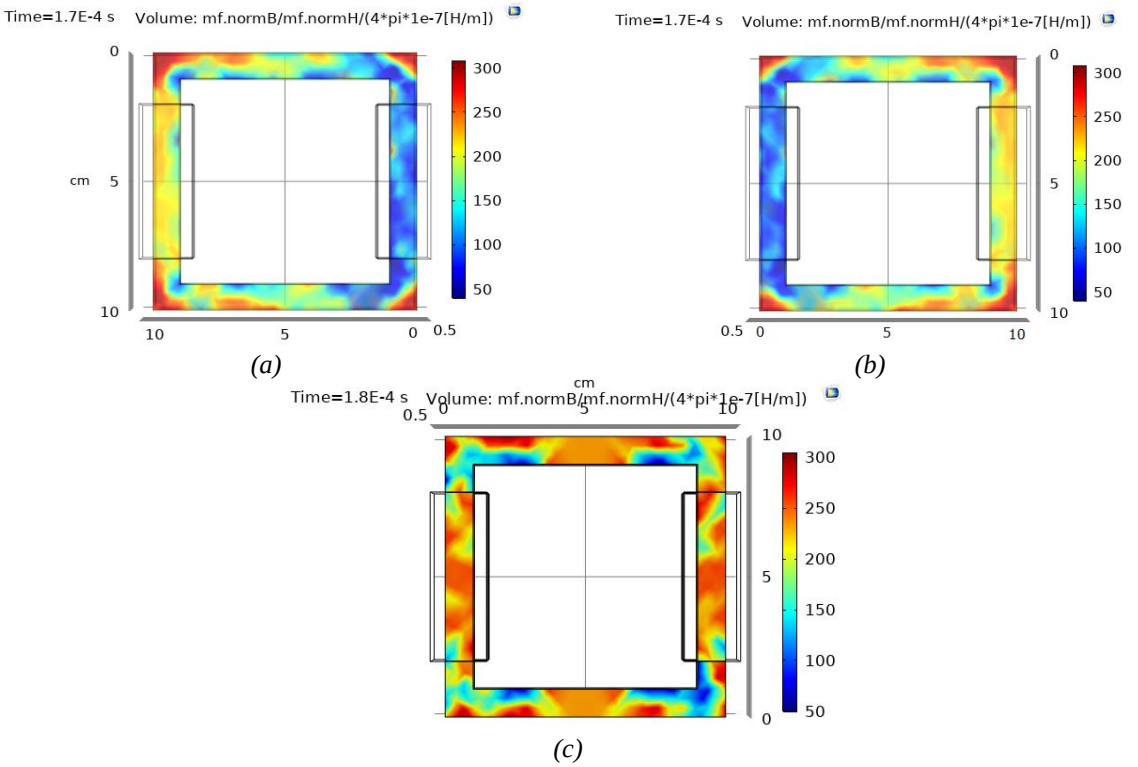

Figure 6. The magnetic permeability of the fluid core: a) Primary winding is powered on b) Secondary winding is powered on, c) Both windings are on with the same current excitation.

The magnetic field strength (*H*) and the magnetization norm (*M*) formed in designed MFCT are given in Figs. 7 and 8, respectively. As mentioned, the obtained results are admissible for the powering scheme illustrated.

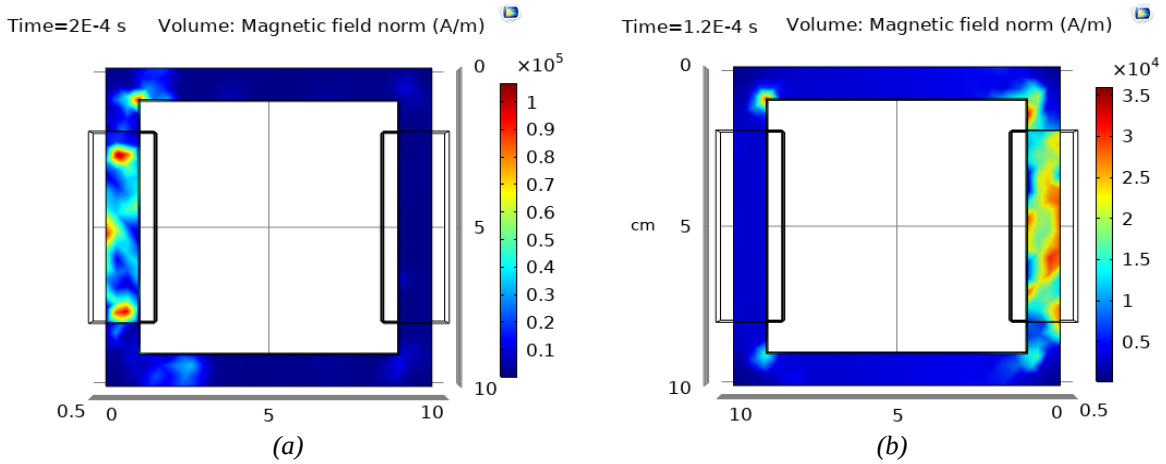

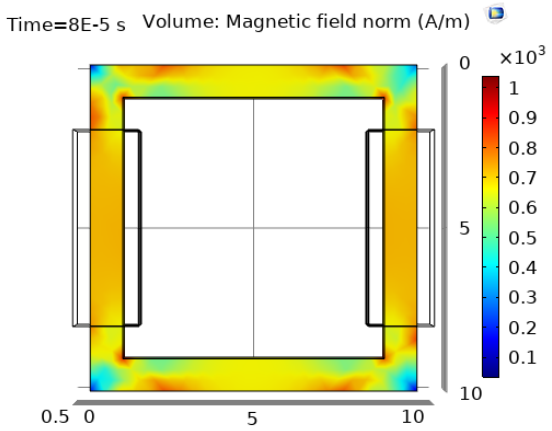

(c)

Figure 7. The magnetic field strength formed in designed MFCT: a) Primary winding is powered on, b) Secondary winding is powered on, c) Both windings are on with the same current excitation.

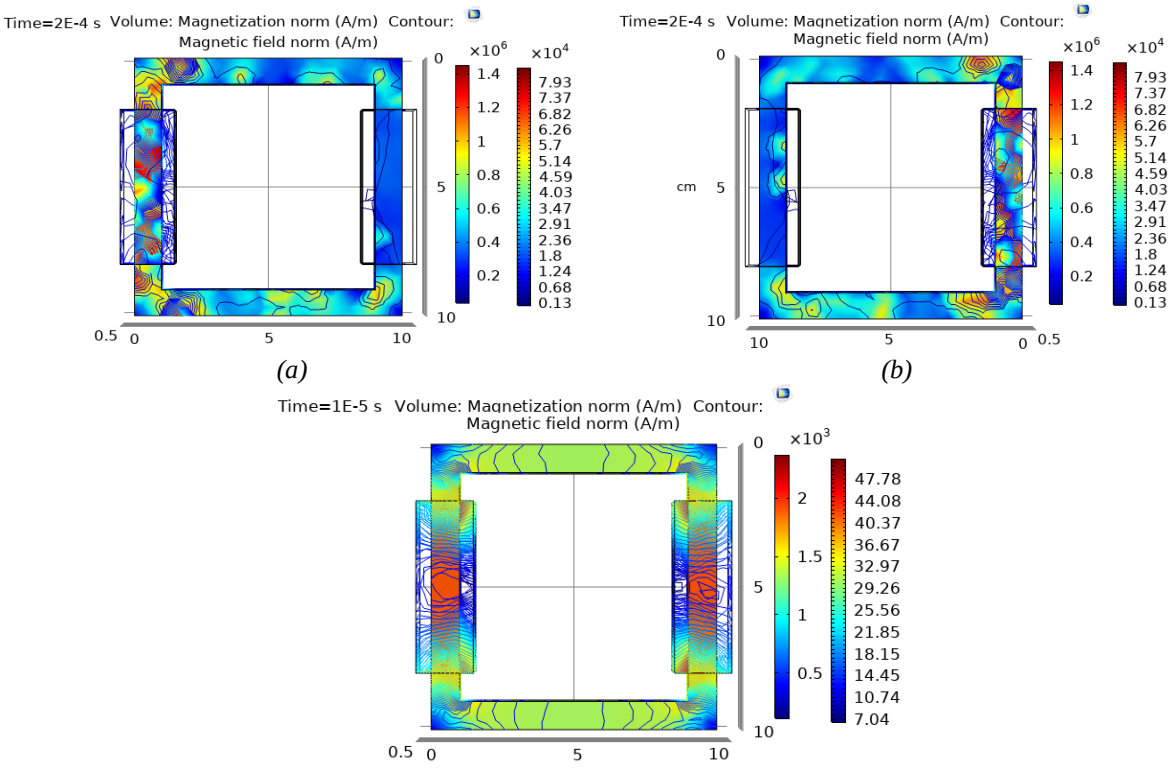

(a) *(b)*

(c)

Figure 8. The magnetization in the designed MFCT: a) Primary winding is powered on, b) secondary winding is powered on, c) both windings are on with the same current excitation.

In order to obtain the results of magnetic fields and turbulent flow modules simultaneously, both physics are applied to the same study in simulation model. As a result, it is possible to observe the flow patterns created in MFCT's core by applying magnetic forces. Stream tubes depict the flow field, and their color and size are related to the velocity module. It should be noticed that the mass concentration of the particles floating in fluids is constant for the simulation model. Therefore, the magnetization body forces that entrain the flow are not different. Fig. 9 presents 3D views of the velocity field (v) and Fig. 10 indicates the pressure (P) through the core as both physics are applied.

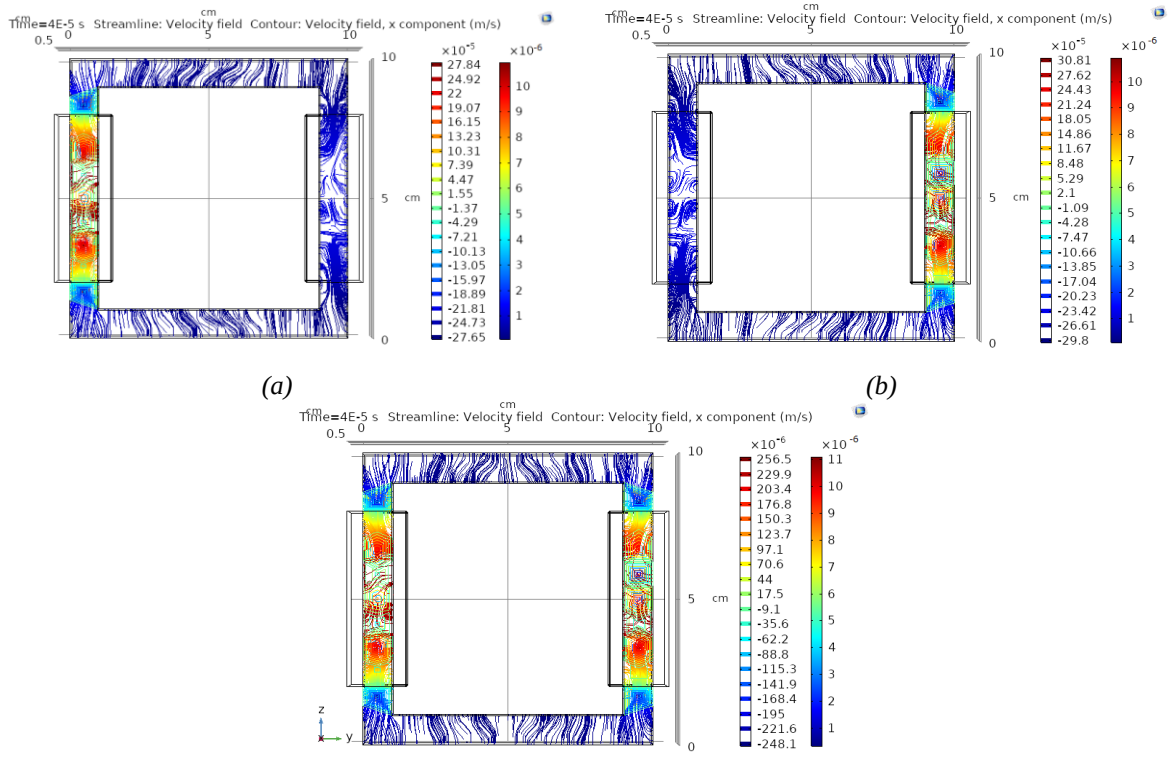

(a) *(b)*

(c)

Figure 9. Stream tubes showing the velocity field patterns of the model: a) Primary winding is powered on, b) secondary winding is powered on, c) both windings are on with the same current excitation.

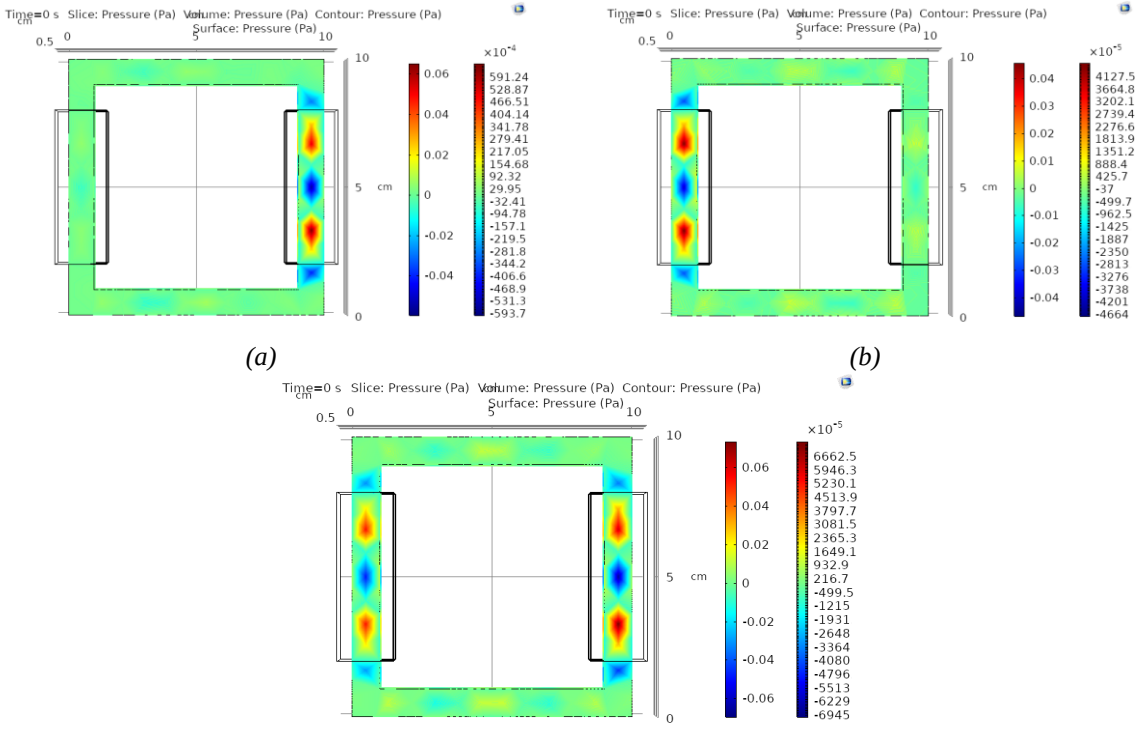

(a) *(b)*

(c)

Figure 10. Pressure patterns for different powering schemes of the model: a) Primary winding is powered on b) Secondary winding is powered on, c) Both windings are on with the same current excitation.

The magnetic flux densities and the flowing fluxes for primary winding excitation with an identical AC current are indicated through flux lines. Since the study is time dependent, the magnetic flux density

produced is varying with respect to time. In this case, the MFCT contains a core with 50% mass fraction of magnetic nanoparticles (ρ =4336.25 [kg/m^3] mixture density).

According to Fig. 11 it is obvious that the current excitation applied to primary winding for t=0.14 ms, t=0.15 ms and t=0.16 ms leads to different values of flux density. Because the MFCT is considered as a step-up transformer, an increment is observed in the flux lines of secondary winding side. The magnetic flux density component for x, y and z directions are indicated in Fig. 12. The flux density has more quantities in x direction with comparison to y and z. This issue is directly dependent on the geometry defined for the transformer.

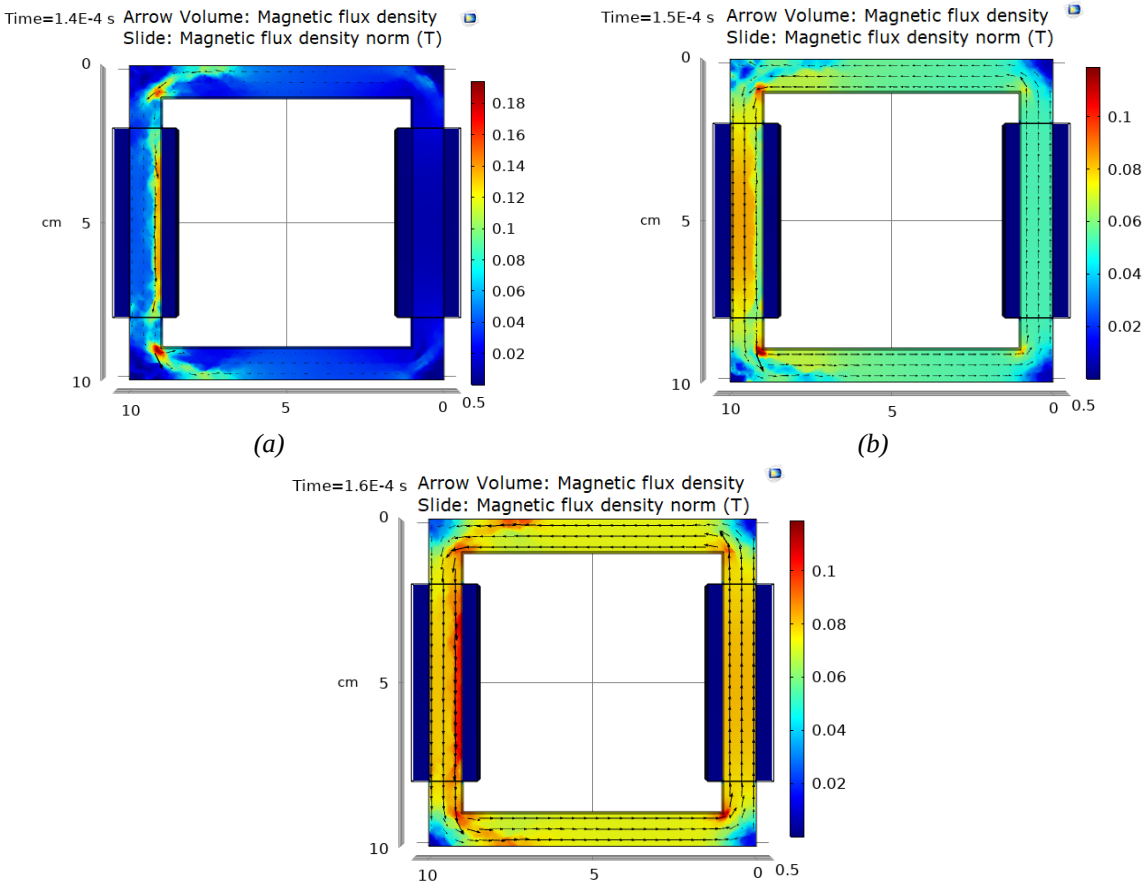

(a) *(b)*

(c)

Figure 11. The magnetic flux densities and the flowing flux for a) t=0.14ms, b) t=0.15ms, c) t=0.16ms.

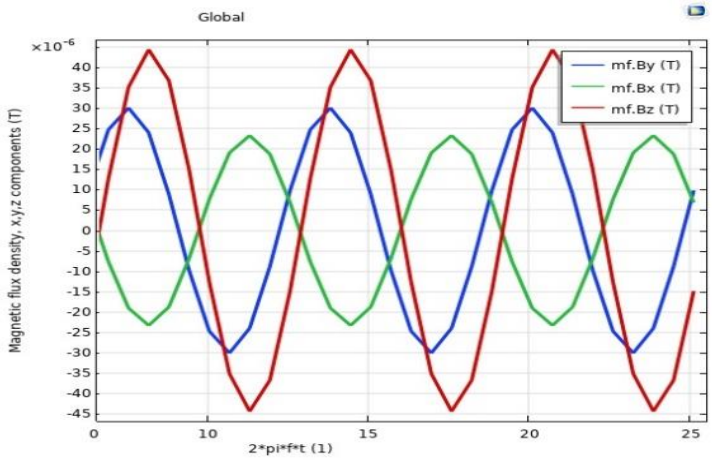

Figure 12. The generated magnetic flux density components.

The parameters and descriptions defined for designed transformer are given in Table 3.

Table 3. The MFCT parameters and descriptions

Parameter	Description
Core geometry (x) (cm)	2
Core geometry (y) (cm)	2
Core geometry (z) (cm)	6
Primary winding	10
Secondary winding	80
Coil type	Numeric
Coil wire conductivity[S/m]	(60) (10^7)
Conductor model	Homogenized multi-turn
Coil wire cross section area (m2)	10^{-6}
Coil excitation	$5V_{p\text{-}p}$

In order to obtain the relationship between simulation parameters and the output characteristics of the model, the second phase of the simulation study is processed. In this phase, all parameters but the dispersed phase concentration φ_d are the same as the previous study. Following the simulation steps, the *B-H* curves for various concentrations of dispersed phase φ_d in the same carrier are evaluated and plotted in Fig. 13. The concentration rate has a percentage quantity between 10% and 90%. As the percentage raises, the saturation magnetization increases for the same amount of magnetic flux intensities applied.

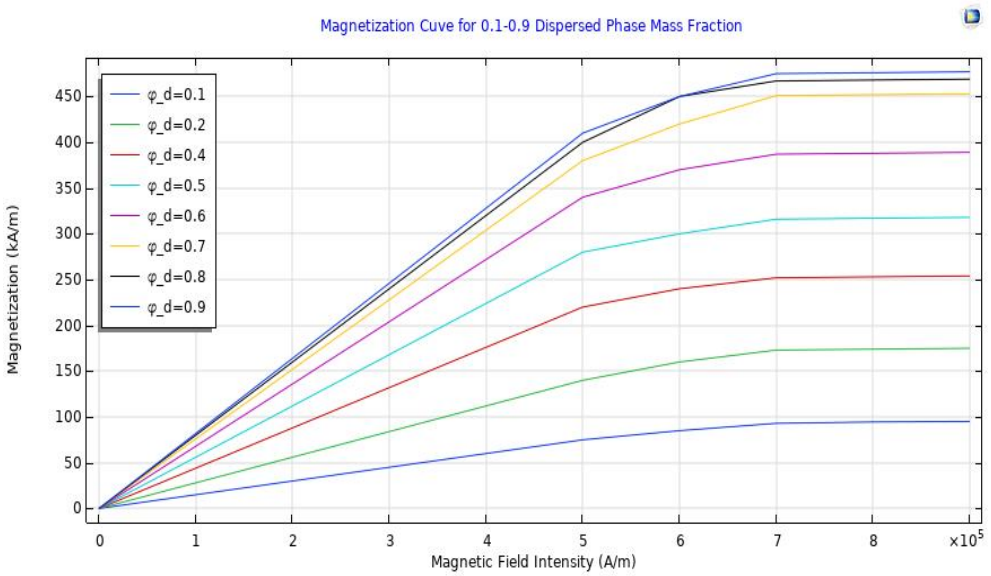

Figure 13. The magnetization curve generated for various concentration rates of the magnetic fluid.

It is important to notice that these evaluations and plots are enhanced for a special operating frequency of MFCT operation. Hence, it can be concluded that the secondary winding voltages exhibit different behavior with respect to frequency and primary winding voltage. The waveforms of the secondary winding voltage by raising the iron powder mass concentration for the case when a 4 Ω resistor is connected to the secondary winding are presented in Fig. 14.

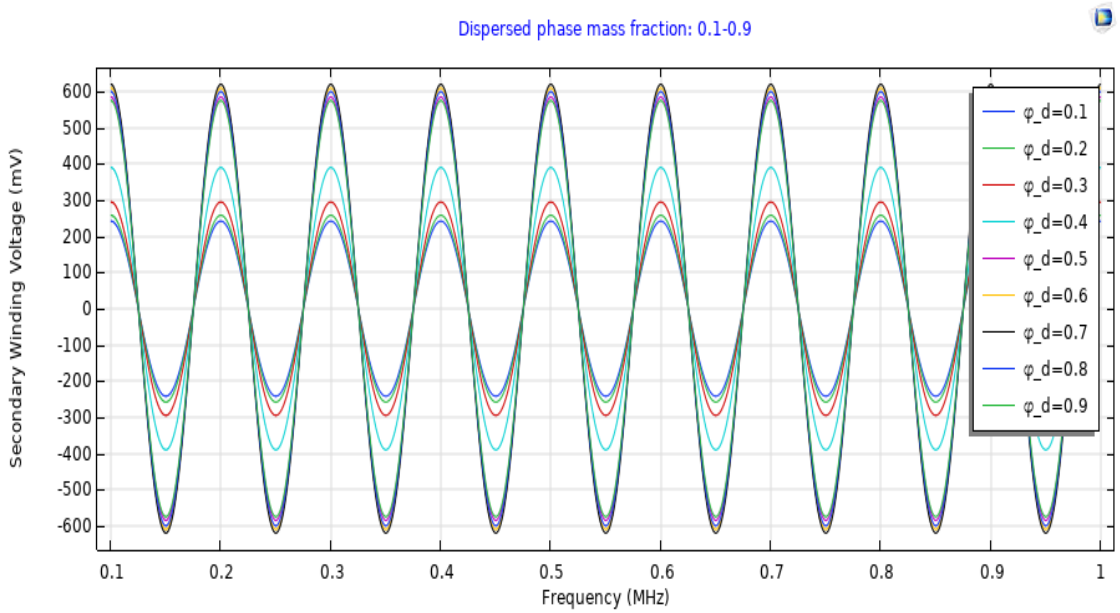

Figure 14. The secondary winding voltage waveforms for various dispersed phase mass fraction of the magnetic fluid.

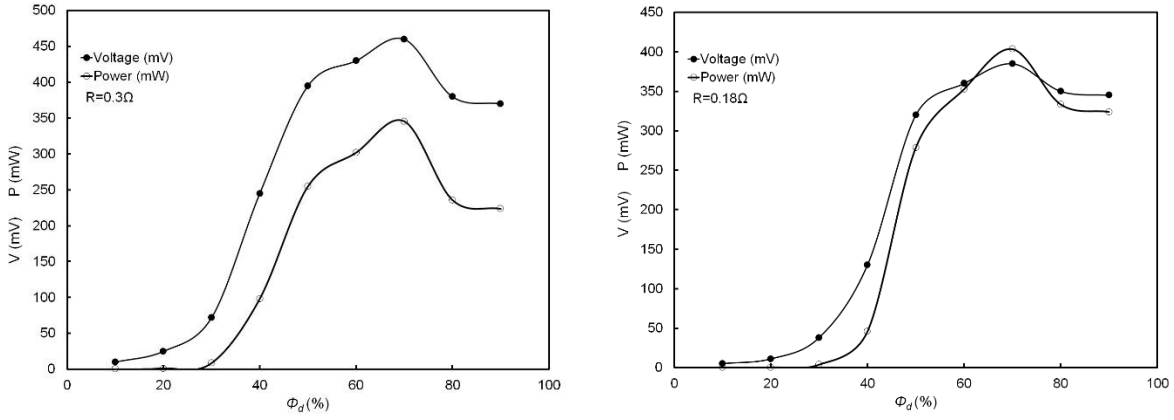

(a) *(b)*

Figure 15. The secondary winding voltage and power for various mass fraction of magnetic particles in the magnetic fluid. The electrical loads of secondary windings are (a) R= 0.3 Ω and (b) R= 0.18 Ω, respectively.

According to simulation results, the output voltage and power rise with respect to increased magnetic particles mass fraction for 5 *V* peak-to-peak input voltage applied to primary winding. However, the voltage amplitude decays, when the magnetic particle mass is increased further as depicted in Figs. 15(a,b). The optimum power obtained from the secondary windings is also an important issue due to the impedance matching. While the results of Fig. 15(a) are higher than the ones in Fig. 15(b), we can conclude that the electrical load R=0.3 Ω is matched by the impedance of transformer. This fact proves that there exists an optimum amount of magnetic particle mass fraction, which yields to the maximal flux variation by time for the core and that is strictly dependent on the iron powder ratio. In other words, the magnetic characteristics of the core experiences an enhancement by increasing the magnetic property of the liquid.

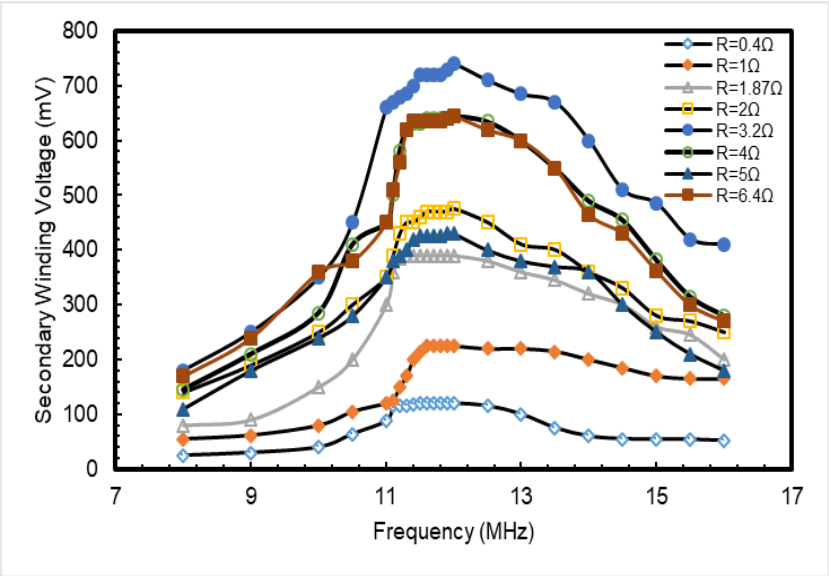

Figure 16. The output voltage characteristics with respect to frequency for various electrical loads attached to the secondary windings.

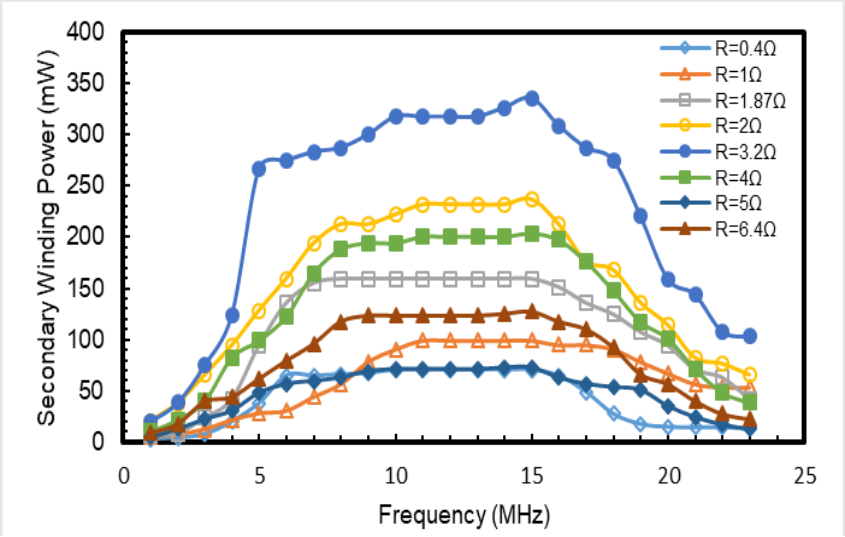

Figure 17. The output power characteristics with respect to frequency for various loads attached to the secondary windings.

It is obvious that the output voltage and power increase with respect to increasing load, although after reaching the maximum frequency rage (around f=12 MHz) the output voltage and hence the output power starts to decay. The maximum output power is obtained for R=3.2 Ω. Consequently, the operating characteristics (i.e. output voltage and power) of the MFCT vary particularly well in 9-13 MHz frequency range while adding various loads to secondary side as they are depicted in Figs. 16 and 17, respectively. The major advantage of changing the magnetic property by raising the magnetite concentration inside the fluid is that there is no permanent magnetization in the hysteresis of the magnetic fluids. The disadvantage is the increase in the magnetic particle concentration and the increase of energy losses in the core at high frequencies (i.e. MHz). However, the effect of this increase on the output characteristics of the transformer in weak power transformers should be examined and evaluated separately. In addition, different doses of magnetic nanoparticles in carrier fluid also change the classical meaning of these fluids.

5. CONCLUSION

In order to reduce the eddy currents and core losses encountered in conventional transformers, the magnetic fluid core transformer (MFCT) is proposed in this paper. Since, magnetic fluid (ferrofluid) core carries the advantages of low conductivity (σ =1.5x10^7 S/m) and super para-magnetism of oil-base magnetic fluidity simultaneously. The mathematical model and the numerical simulations of the transformer with windings are analyzed systematically. The study is concerned with different electric powering schemes providing the operational conditions considered and 3D models are used to compute the magnetic field, the magnetic fluid core flow and magnetic parameters of the MFCT. The magnetic core is a stable, colloidal suspension of magnetic nanoparticles, dispersed in a fluid carrier with engine oil. The magnetization body forces occurring in the MFCT's core result in a turbulent flow and the structure of the flow depends on the magnetic field generated and leads by the powering scheme. Several cells for flowing patterns are created by magnetization of ferrofluid. The flowing physics type is turbulent and Wilcox k–ω model is used to solve them. According to the simulation results, with varying applied frequency values, the most stable frequency range where the MFCT operates, is 9-13 MHz. Future works include the determination of experimental analysis for MFCT by examining several magnetic nanoparticle-oil suspensions with the distinct concentration of magnetic nanoparticles in the base fluid, in order to enhance the best operating results in terms of magnetic flux density production, obtain the optimal magnetic body forces, and hence attain the best magnetization level of MFCT. Thus, in the frame of the present results, instead of using expensive magnetic fluids, cheap and efficient magnetic fluid cores can be replaced for several manufacturing purposes.

REFERENCES

[1] Erickson, RW. Fundamentals of Power Electronics, 2nd Edition. Norwell, Massachusetts USA: Springer International Edition, 2001.

[2] Colonel, W, McLyman, T. Transformer and Inductor Design Handbook, 3rd edition. New York U.S.A: Marcel Dekker, 2004.

[3] Balcı, S. Nanokristal nüve malzemesi ile orta frekans güç transformatörünün analizi, tasarımı ve gerçekleştirilmesi [Analysis, design and realization of medium frequency power transformer with nanocrystalline core material] (PhD). Gazi Üniversitesi, Ankara, Turkey, 2016.

[4] Kul, S, Iskender I, Balci, S. FEA Simulation of the Electromagnetic Effects on the Flux Distribution of the Joints in the Transformer Core Structure. In: ISMSIT 2018 2nd International Symposium on Multidisciplinary Studies and Innovative Technologies; 2018: IEEE, pp. 1-5, doi: 10.1109/ISMSIT.2018.8566684.

[5] Isa, M Z, Kadir, A, Gomes, C, Azis, N, Izadi, M, Alyozbaky, OSH. Analysis on magnetic flux density and core loss for hexagonal and butt-lap core joint transformers. In: SPEC 2016 IEEE 2nd Annual Southern Power Electronics Conference; 5-8 Dec 2016: IEEE, Auckland, New Zealand, pp. 1-4.

[6] Tomczuk, B, Koteras, D. Magnetic flux distribution in the amorphous modular transformers. Journal of Magnetism and Magnetic Materials 2011; 323(12): 1611-1615. DOI:10.1016/j.jmmm.2011.01.007.

[7] Yıldırız, E, Aydemir, MT. Küçük güçlü bir rüzgar jenaratöründe kullanım için eksenel akıllı bir sürekli mıknatıslı motorun analizi, tasarımı ve gerçekleştirilmesi [Analysis, design and realization of an axial intelligent permanent magnet motor for use in a small powerful wind generator]. Gazi Üniv.Müh.Mim.Fak.Dergisi 2009; 24 (3): 525-531.

[8] Hasegawa, R, Azuma, D. Impacts of amorphous metal-based transformers on energy efficiency and environment, Journal of Magnetism and Magnetic Materials 2008; 320 (20): 2451-2456. DOI: 10.1016/j.jmmm.2008.04.052

[9] Hasegawa, HWNg, Lee, RAC, Lowdermilk, LA. Amorphous alloy core distribution transformers. In: Proceedings of the IEEE 1991; 79 (11):1608-1623. DOI: 10.1109/5.118984.